Modulation format identification in heterogeneous fiber-optic networks using artificial neural networks

Faisal Nadeem Khan,[1,2,*] Yudi Zhou,[1] Alan Pak Tao Lau[1], and Chao Lu[1]

[1]*Photonics Research Centre, The Hong Kong Polytechnic University, Hung Hom, Kowloon, Hong Kong China*
[2]*School of Electrical and Electronic Engineering, Engineering Campus, Universiti Sains Malaysia (USM), Penang, Malaysia*
[*]eefaisal.nadeem@eng.usm.my

Abstract: We propose a simple and cost-effective technique for modulation format identification (MFI) in next-generation heterogeneous fiber-optic networks using an artificial neural network (ANN) trained with the features extracted from the asynchronous amplitude histograms (AAHs). Results of numerical simulations conducted for six different widely-used modulation formats at various data rates demonstrate that the proposed technique can effectively classify all these modulation formats with an overall estimation accuracy of 99.6% and also in the presence of various link impairments. The proposed technique employs extremely simple hardware and digital signal processing (DSP) to enable MFI and can also be applied for the identification of other modulation formats at different data rates without necessitating hardware changes.

©2012 Optical Society of America

OCIS codes: (060.1660) Coherent communications; (060.2330) Fiber optics communications; (060.2360) Fiber optics links and subsystems; (060.4510) Optical communications; (060.5060) Phase modulation.

References and links

1. I. T. Monroy, D. Zibar, N. G. Gonzalez, and R. Borkowski, "Cognitive heterogeneous reconfigurable optical networks (CHRON): enabling technologies and techniques," in *2011 13th International Conference on Transparent Optical Networks (ICTON)* (2011), paper Th.A1.2.
2. A. Nag, M. Tornatore, and B. Mukherjee, "Optical network design with mixed line rates and multiple modulation formats," J. Lightwave Technol. **28**(4), 466–475 (2010).
3. D. C. Kilper, R. Bach, D. J. Blumenthal, D. Einstein, T. Landolsi, L. Ostar, M. Preiss, and A. E. Willner, "Optical performance monitoring," J. Lightwave Technol. **22**(1), 294–304 (2004).
4. Z. Pan, C. Yu, and A. E. Willner, "Optical performance monitoring for the next generation optical communication networks," Opt. Fiber Technol. **16**(1), 20–45 (2010).
5. C. K. Chan, *Optical Performance Monitoring* (Academic, 2010).
6. N. Hanik, A. Gladisch, C. Caspar, and B. Strebel, "Application of amplitude histograms to monitor performance of optical channels," Electron. Lett. **35**(5), 403–404 (1999).
7. B. Kozicki, O. Takuya, and T. Hidehiko, "Optical performance monitoring of phase-modulated signals using asynchronous amplitude histogram analysis," J. Lightwave Technol. **26**(10), 1353–1361 (2008).
8. S. D. Dods and T. B. Anderson, "Optical performance monitoring technique using delay tap asynchronous waveform sampling," in *Optical Fiber Communication Conference and Exposition and The National Fiber Optic Engineers Conference*, Technical Digest (CD) (Optical Society of America, 2006), paper OThP5.
9. T. B. Anderson, A. Kowalczyk, K. Clarke, S. D. Dods, D. Hewitt, and J. C. Li, "Multi impairment monitoring for optical networks," J. Lightwave Technol. **27**(16), 3729–3736 (2009).
10. X. Wu, J. A. Jargon, R. A. Skoog, L. Paraschis, and A. E. Willner, "Applications of artificial neural networks in optical performance monitoring," J. Lightwave Technol. **27**(16), 3580–3589 (2009).
11. F. N. Khan, T. S. R. Shen, Y. Zhou, A. P. T. Lau, and C. Lu, "Optical performance monitoring using artificial neural networks trained with empirical moments of asynchronously sampled signal amplitudes," IEEE Photon. Technol. Lett. **24**(12), 982–984 (2012).
12. F. N. Khan, A. P. T. Lau, C. Lu, and P. K. A. Wai, "Chromatic dispersion monitoring for multiple modulation formats and data rates using sideband optical filtering and asynchronous amplitude sampling technique," Opt. Express **19**(2), 1007–1015 (2011).
13. B. Kozicki, A. Maruta, and K. Kitayama, "Transparent performance monitoring of RZ-DQPSK systems employing delay-tap sampling," J. Opt. Netw. **6**(11), 1257–1269 (2007).

14. A. P. T. Lau, Z. Li, F. N. Khan, C. Lu, and P. K. A. Wai, "Analysis of signed chromatic dispersion monitoring by waveform asymmetry for differentially-coherent phase-modulated systems," Opt. Express **19**(5), 4147–4156 (2011).
15. F. N. Khan, A. P. T. Lau, Z. Li, C. Lu, and P. K. A. Wai, "OSNR monitoring for RZ-DQPSK systems using half-symbol delay-tap sampling technique," IEEE Photon. Technol. Lett. **22**(11), 823–825 (2010).
16. F. N. Khan, A. P. T. Lau, Z. Li, C. Lu, and P. K. A. Wai, "Statistical analysis of optical signal-to-noise ratio monitoring using delay-tap sampling," IEEE Photon. Technol. Lett. **22**(3), 149–151 (2010).
17. Y. Zhou, T. B. Anderson, K. Clarke, A. Nirmalathas, and K. L. Lee, "Bit-rate identification using asynchronous delayed sampling," IEEE Photon. Technol. Lett. **21**(13), 893–895 (2009).
18. N. G. Gonzalez, D. Zibar, and I. T. Monroy, "Cognitive digital receiver for burst mode phase modulated radio over fiber links," in *2010 36th European Conference and Exhibition on Optical Communication (ECOC)* (2010.), paper P6.11.
19. E. E. Azzouz and A. K. Nandi, *Automatic Modulation Recognition of Communication Signals* (Kluwer Academic Publishers, Boston, 1996).
20. O. A. Dobre, A. Abdi, Y. Bar-Ness, and W. Su, "A survey of automatic modulation classification techniques: classical approaches and new trends," IET Commun. **1**(2), 137–156 (2007).
21. A. K. Nandi and E. E. Azzouz, "Algorithms for automatic modulation recognition of communication signals," IEEE Trans. Commun. **46**(4), 431–436 (1998).
22. W. Wei and J. M. Mendel, "Maximum-likelihood classification for digital amplitude-phase modulations," IEEE Trans. Commun. **48**(2), 189–193 (2000).
23. W. Su, J. L. Xu, and M. Zhou, "Real-time modulation classification based on maximum-likelihood," IEEE Commun. Lett. **12**(11), 801–803 (2008).
24. A. K. Nandi and E. E. Azzouz, "Modulation recognition using artificial neural networks," Signal Process. **56**(2), 165–175 (1997).
25. Z. Yaqin, R. Guanghui, W. Xuexia, W. Zhilu, and G. Xuemai, "Automatic digital modulation recognition using artificial neural networks," in *Proceedings of the 2003 International Conference on Neural Networks and Signal Processing* (2003), Vol.1, pp. 257–260.
26. M. L. D. Wong and A. K. Nandi, "Automatic digital modulation recognition using spectral and statistical features with multi-layer perceptrons," in *Sixth International, Symposium on Signal Processing and its Applications* (2001.), Vol. 2, pp. 390–393.
27. I. Kaastra and M. Boyd, "Designing a neural network for forecasting financial and economic time series," Neurocomputing **10**(3), 215–236 (1996).
28. H. Yu and B. M. Wilamowski, "Levenberg-Marquardt Training," in *The Industrial Electronics Handbook*, *Vol. 5–Intelligent Systems*, 2nd ed. (CRC Press, Boca Raton, 2011).
29. VPIsystems™, "VPItransmissionMaker™."

1. Introduction

With the emergence of broadband data services such as video-on-demand (VoD), Internet Protocol television (IPTV), multimedia messaging service (MMS), online gaming etc., service providers are experiencing increasing demands to upgrade their networks in order to support these high data rate applications. On the other hand, the service providers are expected to keep supporting some of the existing voice and data services. Therefore, it is envisaged that the future fiber-optic networks will be heterogeneous in nature supporting a wide range of data traffic depending upon the end users' demands [1]. In order to support these heterogeneous services and hence the data traffic, the future fiber-optic networks are anticipated to encompass mixed line rates (MLR) (such as 10/40/100 Gbps) as well as multiple modulation formats [2].

The management of available resources in complex heterogeneous networks will be a challenging task and would require the acquisition of incessant and real-time information about the quality of physical links as well as optical signals and passing on this information to the network management system possibly for impairment-aware routing and/or fault localization and diagnosis. Therefore, optical performance monitoring (OPM) is expected to play a crucial role in the efficient management of heterogeneous fiber-optic networks and fulfilling the quality-of-service (QoS) requirements of end users [3,4]. A plethora of OPM techniques has been proposed in recent years capable of monitoring various link impairments and the quality of optical signals [5]. Some of these techniques have demonstrated monitoring of multiple modulation formats and data rates and hence are suitable for OPM in heterogeneous fiber-optic networks. However, these techniques assume either a prior knowledge of the signal modulation format and data rate or the attainment of this information from the network management system [6–16]. In [17], a technique for the identification of data rates is proposed using asynchronous delay-tap sampling for a few modulation formats

types. However, not much work has been done for the recognition/identification of modulation formats in fiber-optic networks. With increasing heterogeneity and dynamics in optical networks, the modulation formats may differ across neighboring wavelength-division multiplexed (WDM) channels from time to time. Although the modulation format information can be obtained from the upper layer protocols in principle, it is practically not feasible to introduce or rely on additional cross-layer communication for the purpose of OPM at the intermediate network nodes. Therefore, MFI will be indispensable for the application of existing OPM techniques in future optical networks [1]. The information about the actual modulation format type of the signal (obtained through MFI) will enable the OPM devices deployed at the intermediate network nodes to apply a monitoring technique suitable for that specific modulation format. In addition to the need of MFI in OPM devices deployed at the intermediate network nodes, digital coherent receivers in next-generation cognitive heterogeneous fiber-optic networks supporting multiple modulation formats and data rates should also be equipped with MFI capabilities without any a priori information [1]. This will be especially important while choosing an appropriate carrier recovery module in a digital coherent receiver. In [18], the recognition of phase-shift keying (PSK) and quadrature amplitude modulation (QAM) signals in digital coherent receivers is demonstrated for radio-over-fiber systems. Due to high cost of a full-fledged coherent receiver with symbol rate sampling, such technique may not be ideal for MFI in OPM devices deployed at the intermediate network nodes where cost is a major constraint.

Modulation recognition has been a topic of extensive research in the digital communications field for the last two decades in applications like static modems, mobile telephony, software defined radio (SDR) etc. and several different techniques have been proposed [19–26]. These techniques can be classified into likelihood-based (LB) and feature-based (FB) approaches. In the LB approach, probabilistic and hypothesis testing arguments are used to formulate the modulation classification problem. This method requires the formulation of correct hypotheses as well as a careful selection of the appropriate threshold values [22,23]. In the FB techniques, on the other hand, prominent features are extracted from the received signal and these features are then utilized for the identification of signal modulation format [24–26]. The LB techniques minimize the probability of false classification and hence provide optimal solution in the Bayesian sense. However, these techniques involve much higher computational complexity. The FB approaches, even though suboptimal, are usually simpler and these techniques can deliver near-optimal performance if designed properly [20]. Both of these approaches have been successfully employed for MFI in copper wire/wireless communications with reasonably good accuracies [19]. However, not much work has been done for MFI in heterogeneous fiber-optic communication networks.

In this paper, we propose a simple and cost-effective FB classification technique for MFI in heterogeneous fiber-optic networks by using an ANN trained with the features extracted from AAHs [6] of the directly detected signals. Numerical simulations have been performed for six different widely-used modulation formats at various data rates, namely 10 Gbps return-to-zero (RZ) on-off keying (OOK), 40 Gbps non-return-to-zero (NRZ) differential phase-shift keying (DPSK), 40 Gbps optical duobinary (ODB), 40 Gbps RZ differential quadrature phase-shift keying (DQPSK), 100 Gbps polarization-multiplexed (PM) RZ quadrature phase-shift keying (QPSK) and 200 Gbps PM-NRZ 16 quadrature amplitude modulation (16QAM) for optical signal-to-noise ratio (OSNR) values as low as 12 dB and chromatic dispersion (CD) and differential group delay (DGD) in the ranges of −500−500 ps/nm and 0−10 ps respectively. The simulations results demonstrate successful identification of all modulation formats with an overall estimation accuracy as high as 99.6%. The proposed technique can be used in digital coherent receivers for the recognition of unknown transmitted modulation formats, which will be one of the major tasks in next-generation intelligent receivers. Due to its implementation simplicity, it can also be used for MFI in OPM devices deployed at the intermediate network nodes which can only afford limited complexity. Hence, the proposed technique can enable the application of existing OPM techniques in future heterogeneous fiber-optic networks. Furthermore, since only asynchronous amplitude samples
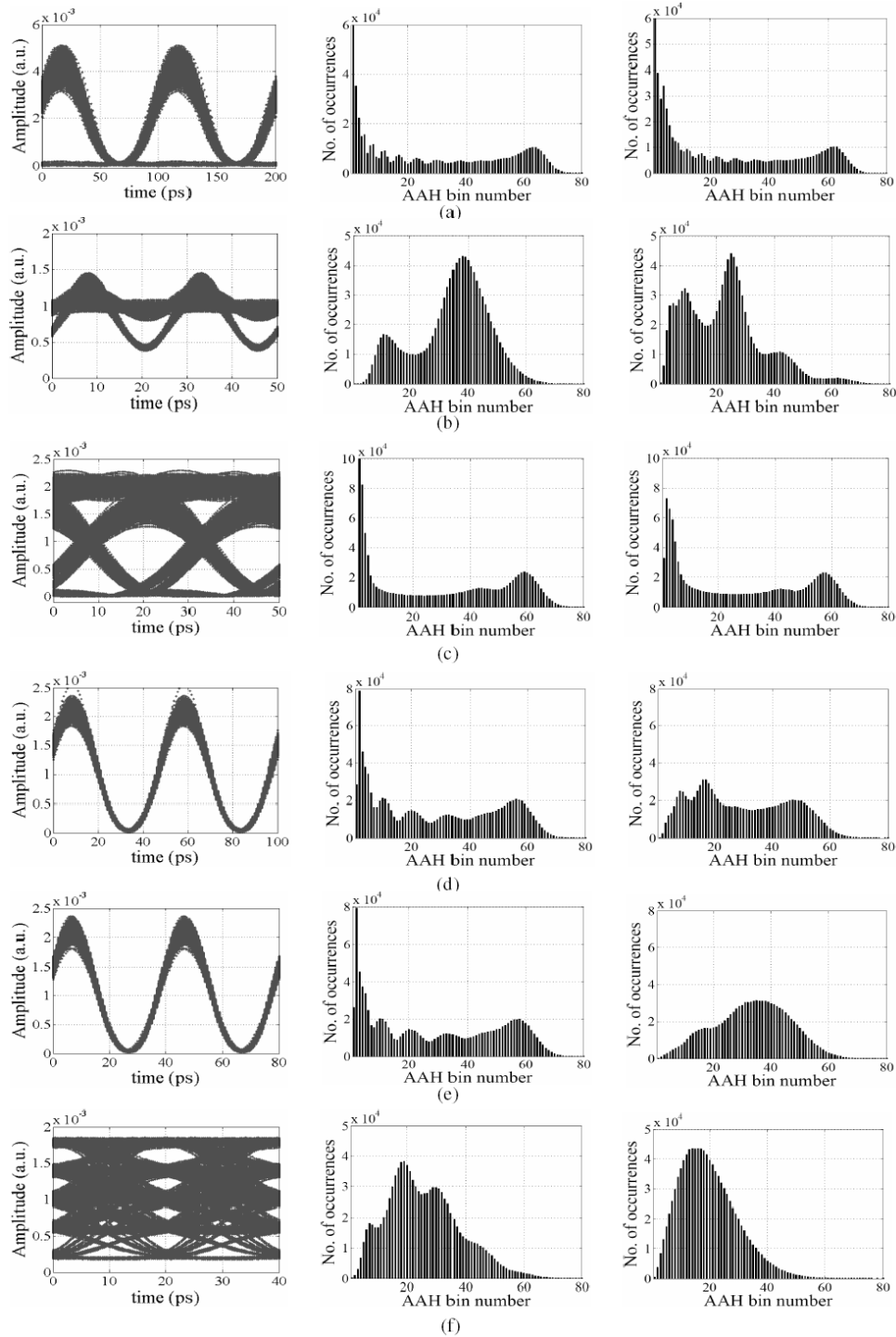
Fig. 1. Eye-diagrams and corresponding AAHs for (a) 10 Gbps RZ-OOK, (b) 40 Gbps NRZ-DPSK, (c) 40 Gbps ODB, (d) 40 Gbps RZ-DQPSK, (e) 100 Gbps PM-RZ-QPSK and (f) 200 Gbps PM-NRZ-16QAM formats after direct detection. The second column shows the AAHs for OSNR = 18 dB, neither CD nor PMD while the third column shows the AAHs for OSNR = 18 dB, CD = 100 ps/nm and DGD = 5 ps when the signal's state-of-polarization (SOP) is 45° with respect to the principal states-of-polarization (PSP) of the PMD emulator.

are needed, the proposed technique can enable the recognition of multiple modulation formats at various data rates without necessitating hardware changes.

2. MFI using ANN trained with AAHs

The eye-diagrams and corresponding AAHs of the directly detected signals for various commonly-used modulation formats in long-haul optical communication systems are shown in Fig. 1. It is clear from the figure that different modulation formats exhibit distinct pulse shapes after direct detection (as obvious from their eye-diagrams). Consequently, the AAHs of these modulation formats will also be unique and exhibit distinct signatures for various formats. The AAHs change significantly with various link impairments but they still remain different from each other and hence are distinguishable as evident from the second and third columns of Fig. 1. The characteristic features of AAHs can thus be exploited for the identification of respective modulation formats using the FB classification techniques employing ANNs, which are widely accepted as universal classifiers. ANNs are information processing systems and are comprised of several layers of processing elements called neurons. The neurons in two adjacent layers are interlinked and have variable strength (called weight) for each connection as shown in Fig. 2.
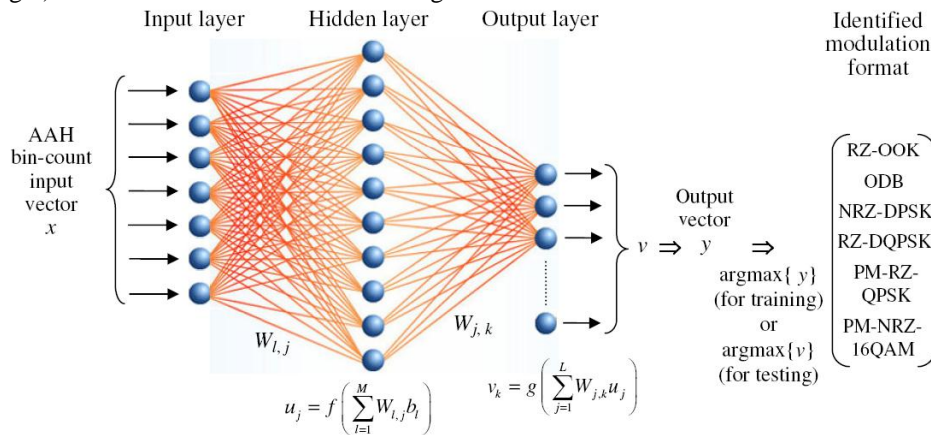

Fig. 2. Structure of an MLP3-ANN with AAH bin-count vector x as input and estimated modulation format type vector y as output.

Neural networks-based classification processes typically involve the selection of suitable ANN architectures and appropriate learning algorithms in order to achieve the desired classification accuracies. In our proposed technique, the AAHs of directly detected signals, which are represented by M x 1 vectors of bin-counts x, are used as inputs. In the training phase of ANN, each input vector x has a corresponding N x 1 binary vector y with only one non-zero element. The location of '1' in y, or argmax$\{y\}$, indicates the signal modulation format type. Due to the analogue nature of ANN, the ANN output v can only be trained close to but not identical to y. In fact, various ANN parameters are optimized during the training process to minimize the mean-square-error (MSE) $\|v - y\|^2$ over the whole training data set. In the testing phase, argmax$\{v\}$ is used as an identifier of the signal modulation format. An example showing the relationship between x, v, y and the signal modulation format type in the proposed ANN-based MFI technique is shown in Fig. 3.

The ANN architecture used in our simulations is a 3-layer multilayer perceptron (MLP3) neural network consisting of an input layer, one hidden layer and an output layer as shown in Fig. 2. The selection of one hidden layer for the ANN is a practical choice since increasing the number of hidden layers results in an increase in computation time and it may also enhance the risk of over-fitting. Theoretically, an ANN with one hidden layer having a
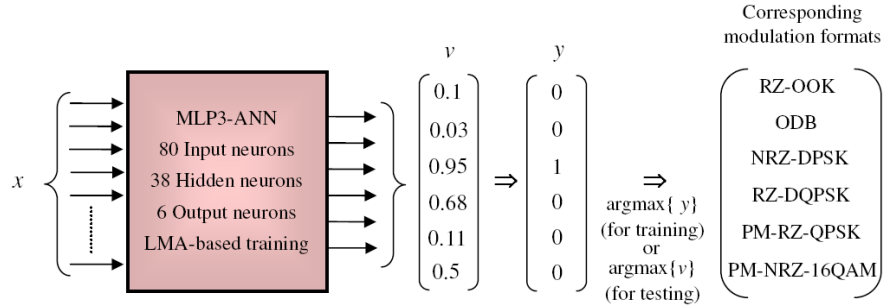
Fig. 3. An example illustrating the relationship between *x, v, y* and the signal modulation format type. In the training phase, for each input *x*, the corresponding binary vector *y* contains a '1' and all zeros. The location of '1' in *y*, or argmax{*y*}, indicates the signal modulation format. The ANN attempts to minimize the MSE between *y* and the analogue ANN output *v*. In the testing phase, argmax{*v*} is used as an identifier of the signal modulation format.

sufficient number of neurons can approximate any continuous function. This is the reason why ANNs comprised of one or occasionally two hidden layers are commonly used in practice [27]. In our case, the number of neurons in the input and output layers are determined by the number of AAH bins and the number of modulation formats types respectively and hence, we have chosen them to be 80 and 6 neurons respectively. A supervised learning method called back-propagation (BP) [27] is employed for the training of ANN. The number of neurons in the hidden layer is optimized to be 38 using the incremental-constructive approach where the number of neurons is increased iteratively until the MSE performance deteriorates. The activation functions $f(.)$ and $g(.)$, also referred to as transfer or threshold functions, are then selected for the hidden and output layers neurons. We have used a tangent sigmoid activation function given by $f(z) = (e^z - e^{-z})/(e^z + e^{-z})$ for the hidden layer neurons and a linear activation function given by $g(z) = z$ for the output layer neurons, where z is the input to a hidden or output layer neuron. The overall data set comprised of 26,208 input/output vector pairs $[X,Y] = \{[x_1,y_1], [x_2,y_2], ... [x_S,y_S]\}$, where $S = 26,208$ is the size of overall data set, is divided into three distinct subsets namely training, validation and testing data sets. The sizes of these three subsets are chosen to be 56%, 19% and 25% respectively of the overall data set while the individual input/output vector pairs of each of these three subsets are randomly selected from the overall data set. The training data set $[X_{Train},Y_{Train}]$ is used to optimize the ANN parameters so as to minimize the MSE $\|v_i - y_i\|^2$ over the whole training data set. We have used the popular Levenberg-Marquardt algorithm (LMA) for the ANN training process due to its fast convergence speed, robustness and its suitability to medium-sized nonlinear models [28]. Figure 4 shows the MSE during the training phase as a function of number of epochs. An epoch is a step in the ANN training process in which the whole training data set is presented once to the ANN for learning and network parameters optimization. It is evident from the figure that the MSE decreases with an increase in number of epochs for the training data set. During the course of training, a check on the ANN performance is carried out by examining it against the validation data set $[X_{Valid},Y_{Valid}]$ and the over-training of ANN is avoided by enforcing the early termination if the validation data set starts to give higher MSE. As shown in Fig. 4, the minimum MSE of 4.97 x 10^{-3} is achieved for 53 epochs and the training process is aborted there. Once the training and validation phases are over, a testing phase is conducted using the testing data set $[X_{Test},Y_{Test}]$ such that for each input vector x_i, the identified modulation format type i.e. argmax{v_i} is compared with the correct type and the number of erroneous identifications as well as overall success rate is determined.
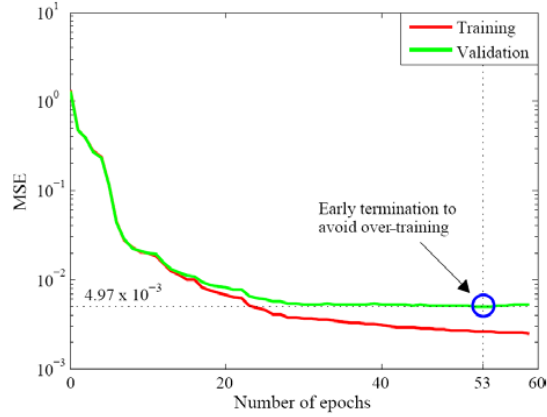
Fig. 4. Dependence of MSE on the number of epochs for the training and validation data sets. Best validation performance at MSE = 4.97 x 10^{-3} is achieved for 53 epochs and the training process is then terminated.
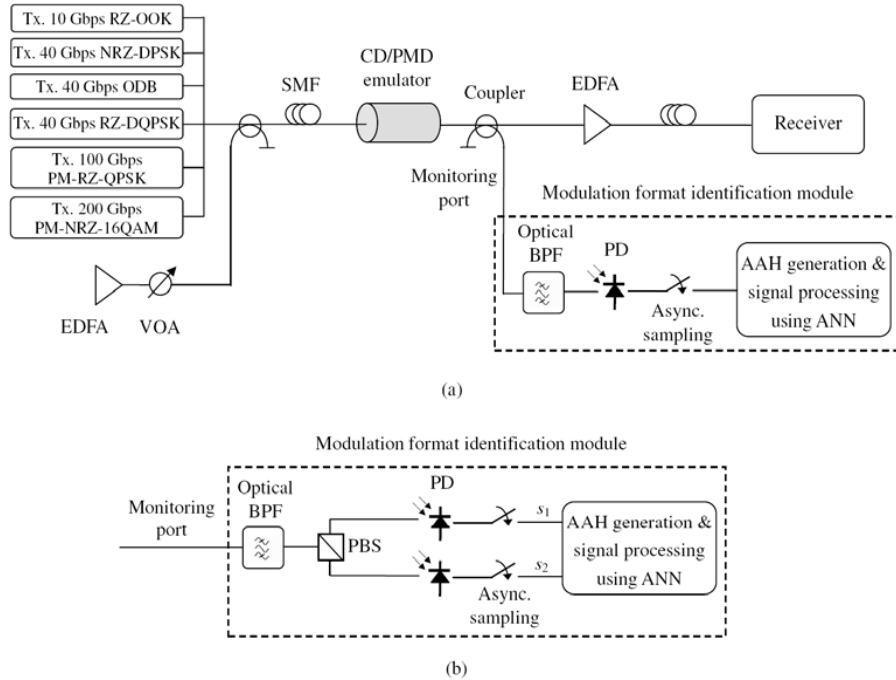

Fig. 5. (a) System configuration for MFI using ANN trained with AAHs. (b) Modified MFI configuration for distinguishing between the RZ-DQPSK and PM-RZ-QPSK formats for small CD and DGD values.

3. System configuration, results and discussion

To demonstrate the validity of the proposed MFI technique using ANN, numerical simulations are performed using the commercial software VPI [29]. The simulation setup is shown in Fig. 5. Six different commonly-used modulation formats at various data rates i.e. 10
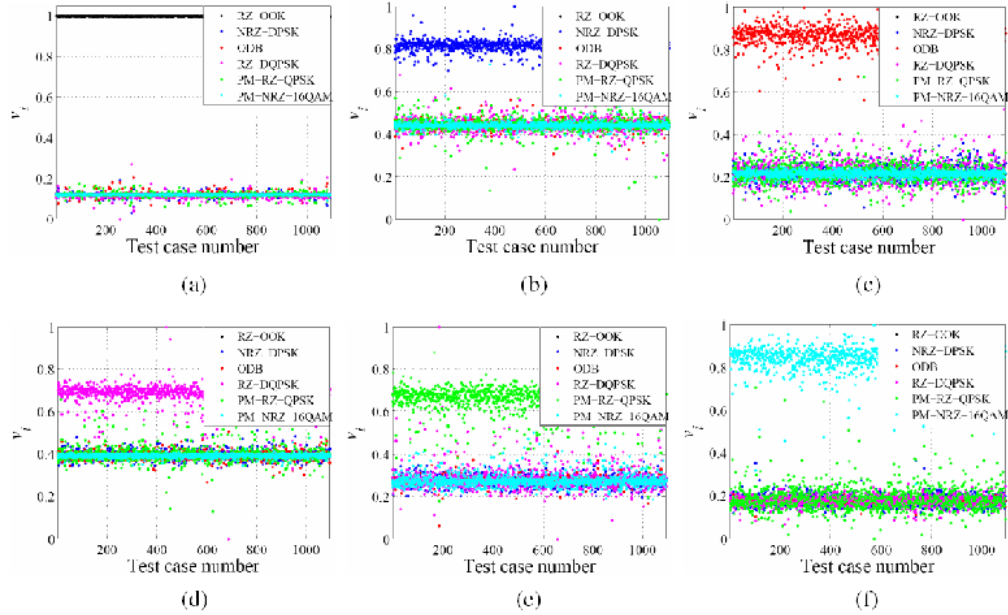
Fig. 6. The six elements of the ANN outputs v_i corresponding to (a) 10 Gbps RZ-OOK, (b) 40 Gbps NRZ-DPSK, (c) 40 Gbps ODB, (d) 40 Gbps RZ-DQPSK, (e) 100 Gbps PM-RZ-QPSK and (f) 200 Gbps PM-NRZ-16QAM modulation formats for the testing data set containing 6552 test cases randomly drawn from the overall data set and corresponding to different OSNR, CD, DGD and polarization angle values.

Gbps RZ-OOK, 40 Gbps NRZ-DPSK, 40 Gbps ODB, 40 Gbps RZ-DQPSK, 100 Gbps PM-RZ-QPSK and 200 Gbps PM-NRZ-16QAM are generated and transmitted over a single-mode fiber (SMF). An erbium-doped fiber amplifier (EDFA) is used to add amplified spontaneous emission (ASE) noise into the signal and a variable optical attenuator (VOA) is used to adjust the OSNR in the range between 12 and 26 dB. A CD and first-order polarization-mode dispersion (PMD) emulator is used to introduce variable amounts of CD and DGD into the signal respectively. The CD is introduced in the range between −500 and 500 ps/nm in steps of 80 ps/nm while DGD is introduced in the range between 0 and 10 ps in steps of 2 ps. The launching angle α of the transmitted signal's SOP with respect to the PSP of the PMD emulator is varied randomly. For monitoring purposes, a fraction of the signal is tapped from the optical link and is fed into the MFI module where the desired channel is filtered using an optical band-pass filter (BPF) and afterwards directly detected using a photodetector (PD) (the optical and electrical bandwidths of the receiver in our simulations are 0.8 nm and 50 GHz respectively). The resulting electrical signal is asynchronously sampled at a rate much slower than the symbol rates of all the modulation formats to obtain 200,000 amplitude samples, which are then used to form AAH containing 80 bins. A large data set comprised of 26,208 such AAHs is generated corresponding to different OSNR, CD, DGD, α and modulation formats types and the randomly selected subsets of this large data set are then used for training, validation and testing of ANN as described in the previous section.

The six elements of the ANN outputs v_i for the testing data set comprised of 6552 input/output vector pairs (randomly selected from the overall data set) are shown in Fig. 6. It is clear from the figure that one particular element in v_i is considerably larger than the others in almost all the cases, thus suggesting that the modulation formats are clearly and easily identified. The differences in the elements of v_i are larger for RZ-OOK, ODB and PM-NRZ-16QAM formats as shown in Figs. 6(a), 6(c) and 6(f) and hence, better estimation accuracies can be predicted for these three modulation formats. For NRZ-DPSK format, though the differences in the ANN output values are not quite large, the values are not overlapping as shown in Fig. 6(b) and hence, we can also expect good estimation accuracy for this

modulation format. On the other hand, the elements in v_i corresponding to RZ-DQPSK and PM-RZ-QPSK formats are relatively close to the ones for other formats and there are also overlappings in some cases as shown in Figs. 6(d) and 6(e). Therefore, a few identification errors are anticipated for these two modulation formats. This is due to the fact that the pulse shapes and hence the AAHs of these two modulation formats are quite similar when CD and DGD are small as shown in Figs. 1(d) and 1(e). The overall results for the MFI configuration using the ANN-based classifier only (shown in Fig. 5(a)) are summarized in Table 1. It is clear from the table that all the modulation formats have been well classified with an overall accuracy of 99.06% despite a considerable range of OSNR, CD and DGD. It should be noted that as compared to other modulation formats, the estimation accuracies are relatively bad for RZ-DQPSK and PM-RZ-QPSK formats (i.e. 97.98% and 97.34% respectively) as anticipated.

Table 1. Estimation accuracies of the proposed MFI technique using ANN trained with AAHs and using the setup shown in Fig. 5(a). The overall MFI accuracy is 99.06%.

Actual Modulation Format	Identified Modulation Format					
	RZ-OOK	NRZ-DPSK	ODB	RZ-DQPSK	PM-RZ-QPSK	PM-NRZ-16QAM
RZ-OOK	100%	-	-	-	-	-
NRZ-DPSK	-	99.81%	-	0.18%	-	-
ODB	-	-	99.9%	-	-	-
RZ-DQPSK	-	0.09%	-	97.98%	2.47%	-
PM-RZ-QPSK	-	-	-	1.83%	97.34%	0.64%
PM-NRZ-16QAM	-	0.09%	0.09%	-	0.18%	99.35%

Table 2. Estimation accuracies of the proposed MFI technique using ANN trained with AAHs and exploiting the polarization characteristics of the input signal using the modified MFI configuration shown in Fig. 5(b). The overall MFI accuracy is 99.6%.

Actual Modulation Format	Identified Modulation Format					
	RZ-OOK	NRZ-DPSK	ODB	RZ-DQPSK	PM-RZ-QPSK	PM-NRZ-16QAM
RZ-OOK	100%	-	-	-	-	-
NRZ-DPSK	-	99.81%	-	0.18%	-	-
ODB	-	-	99.9%	-	-	-
RZ-DQPSK	-	0.09%	-	99.17%	0.54%	-
PM-RZ-QPSK	-	-	-	0.64%	99.26%	0.64%
PM-NRZ-16QAM	-	0.09%	0.09%	-	0.18%	99.35%

In order to minimize the ambiguity in the recognition of RZ-DQPSK and PM-RZ-QPSK formats using the ANN-based MFI discussed above, we propose a slightly more sophisticated MFI configuration shown in Fig. 5(b). In this case, the input signal is split into two orthogonal polarization states using a polarization beam splitter (PBS) and the PBS outputs are directly detected independently and then sampled simultaneously but asynchronously to

obtain 200,000 sample pairs (s_1,s_2). Next, the samples s_1 and s_2 are simply added and an AAH of the resulting samples is generated, which is similar to the AAH obtained using a single PD in MFI module shown in Fig. 5(a). In the event that the modulation format is identified to be RZ-DQPSK or PM-RZ-QPSK, the ANN estimates are subjected to further investigations by comparing the average power $E[s_{1(2)}] = P_{1(2)}$ of the individual samples $s_{1(2)}$. In case of single-polarization RZ-DQPSK signal, the splitting of power in PBS depends upon the relative angle between the signal's SOP and the PBS axis (i.e. $P_1 \neq P_2$ for all relative angles between the signal's SOP and the PBS axis except when the angle is 45°) while the signal power will always split equally in PBS (i.e. $P_1 = P_2$) for PM-RZ-QPSK signal. Hence, if $P_1 \neq P_2$, the modulation format is deduced to be RZ-DQPSK. On the contrary, if $P_1 = P_2$, then this could either (most likely) be a PM-RZ-QPSK signal or an RZ-DQPSK signal with 45° relative angle between the signal's SOP and the PBS axis. In this scenario, the additional polarization information is not conclusive and hence, the estimations made by the ANN-based classifier are taken as the final one. Since the AAHs of RZ-DQPSK and PM-RZ-QPSK formats are significantly different from each other unless when CD and DGD are extremely small, the ANN-based classifier itself can well distinguish between these two modulation formats. Fortunately, the joint occurrence of very small CD and DGD and exactly 45° angle between the signal's SOP and PBS axis (in case of RZ-DQPSK signal) is extremely rare and hence, the modified MFI configuration is able to discriminate between these two modulation formats in most of the cases. The results for the modified MFI configuration exploiting such signal polarization characteristics in addition to using the ANN-based classifier (as shown in Fig. 5(b)) are summarized in Table 2. It is evident from the table that the estimation accuracies for RZ-DQPSK and PM-RZ-QPSK formats have been improved using the modified MFI configuration. The overall estimation accuracy for all six modulation formats is also increased to 99.6%, thus signifying the advantage of the modified MFI configuration. We would like to emphasize that the use of this slightly more sophisticated MFI configuration is beneficial only when both RZ-DQPSK and PM-RZ-QPSK modulation formats are present. For all other scenarios, the simple MFI configuration shown in Fig. 5(a) suffices.

The response time of the proposed MFI technique, which is of vital significance in practical applications, is reasonably small. Using a low-cost sampler with 500 Msamples/s sampling rate, the data acquisition time (which takes a bulk of the whole processing time) for 200,000 samples is 0.4 ms. The subsequent generation of AAH from the acquired samples as well as the estimation of modulation format type using ANN can be done comparatively much faster. Note that the training of ANN may take much longer time but such training is performed offline prior to actual MFI process. Hence, we believe that the whole MFI process using the proposed technique can be completed within a few ms at the most in real network settings. If a further reduction in processing time is desired then this can be accomplished by using more than one asynchronous sampling device for the acquisition of amplitude samples.

4. Conclusions

In this paper, we proposed a low-cost MFI technique for next-generation heterogeneous fiber-optic networks by using an ANN trained with the features extracted from AAHs of the directly detected signals. Numerical simulation results demonstrate over 99% identification accuracy for six widely-used modulation formats for OSNR values as low as 12 dB and also in the presence of various levels of CD and PMD. The proposed technique can effectively enable the MFI feature in future receivers as well as in OPM devices deployed throughout the optical network.

Acknowledgments